Chinese Journal of Chemical Engineering 67 (2024) 174–181

Contents lists available at ScienceDirect

Chinese Journal of Chemical Engineering

journal homepage: www.elsevier.com/locate/CJChE

Full Length Article

Effect of surfactant frequently used in soil flushing on oxygen mass transfer in micro-nano-bubble aeration system

Mei Bai [1], Zhibin Liu [1,*], Zhu Liu [1], Chenfei He [1], Zhanhuang Fan [2], Miaoxin Yuan [2]

[1] Jiangsu Key Laboratory of Urban Underground Engineering and Environmental Safety, Southeast University, Nanjing 211189, China
[2] CECEP DADI (Hangzhou) Environmental Remediation Co., Ltd., Hangzhou 310020, China

ARTICLE INFO

Article history:
Received 15 March 2023
Received in revised form
12 November 2023
Accepted 28 November 2023
Available online 7 December 2023

Keywords:
Soil flushing
Micro-nano-bubble aeration
Bio-surfactant
Mass transfer coefficient

ABSTRACT

In-site soil flushing and aeration are the typical synergetic remediation technology for contaminated sites. The surfactant present in flushing solutions is bound to affect the aeration efficiency. The purpose of this study is to evaluate the effect of surfactant frequently used in soil flushing on the oxygen mass transfer in micro-nano-bubble (MNB) aeration system. Firstly, bio-surfactants and chemical surfactants were used to investigate their effects on Sauter mean diameter of bubble (d_{BS}), gas holdup (ε), volumetric mass-transfer coefficient (k_La) and liquid-side mass-transfer coefficient (k_L) in the MNB aeration system. Then, based upon the experimental results, the Sardeing's and Frössling's models were modified to describe the effect of surfactant on k_L in the MNB aeration. The results showed that, for the twenty aqueous surfactant solutions, with the increase in surfactant concentration, the value of d_{BS}, k_La and k_L decreased, while the value of ε and gas-liquid interfacial area (a) increased. These phenomena were mainly attributed to the synergistic effects of immobile bubble surface and the suppression of coalescence in the surfactant solutions. In addition, with the presence of electric charge, MNBs in anionic surfactant solutions were smaller and higher in number than in non-ionic surfactant solutions. Furthermore, the accumulation of surfactant on the gas–liquid interface was more conspicuous for small MNB, so the reduction of k_L in anionic surfactant solutions was larger than that in non-ionic surfactant solutions. Besides, the modified Frössling's model predicted the effect of surfactant on k_L in MNB aeration system with reasonable accuracy.

1. Introduction

Contaminated sites ruin the balance of ecosystem, cause health issues to humans, and are widespread all over the world. Many remediation technologies have been used to achieve an environmentally sound and cost-effective remediation of contaminated sites [1–3]. As a typical one, in-site soil flushing and aeration have always been used synergistically to remediate the contaminated soil and groundwater. At first, flushing solution including surfactant is injected into the contamination region to remove chemical pollutants from the soil. Then, aeration is carried out to introduce oxygen into the groundwater to keep the pollutant-degrading bacteria alive. In this way, the pollutants in groundwater can be removed by metabolic activities of microorganisms. During the process of synergetic remediation, in-site soil flushing and aeration are interrelated. In other words, the surfactant in flushing solution is bound to affect the aeration efficiency.

The effect of surfactant on the oxygen mass transfer during aeration has been widely studied, and it has been found that surfactant always hinders the transfer of oxygen. However, the mechanisms explaining the decrease in oxygen mass transfer are still not well-understood. Various authors have identified the decrease in mass transfer due to hydrodynamic modifications brought by surfactants, such as an increase in the interfacial rigidity that decreases the renewal rates close to the bubble and decreases its terminal velocity [4–6] or a modification of the velocity field surrounding the bubble [7]. Furthermore, the decrease in the oxygen mass transfer due to physicochemical modifications of solution has also been reported [8,9]. These conclusions are based on the study of common bubbles, which occur in conventional aeration process. Recently, fine bubbles have attracted more and more attention. As a typical fine bubble, micro-nano bubble (MNB) with the diameter of less than

* Corresponding author.
E-mail address: seulzb@seu.edu.cn (Z. Liu).

https://doi.org/10.1016/j.cjche.2023.11.009
1004-9541/

200 μm have been widely used in the wastewater treatment systems. However, no correlation with the influence of surfactant on the oxygen mass transfer in MNB aeration was found in present literature. In addition, Painmanakul *et al.* [10] and Sardeing *et al.* [11] found that the effect of surfactant on mass transfer was closely related to the bubble diameter. Rosso and Stenstrom [12] further highlighted that the accumulation of surfactant on the gas–liquid interface of bubble with small diameter was more than that of bubble with larger diameter. Kelsall *et al.* [13], Garner and Hammerton [14], Lee and Kim [15] and Parkinson *et al.* [16] reported that, the smaller the bubble size, the quicker the immobilization of the surface of bubble due to the adsorption of surfactants. Moreover, the studies of Cuenot *et al.* [17] and Takemura [18] revealed that surfactants adsorbed more homogenously on the surface of small bubbles. That is, the effect of surfactants on the oxygen mass transfer for common bubbles is different from that of finer bubbles. Therefore, it is necessary to study the effect of surfactants on the oxygen mass transfer during MNB aeration process.

Over the past decades, related research about the effect of surfactant on the oxygen mass transfer has been done mostly for chemical surfactants. Only a few studies have focused on bio-surfactants. However, bio-surfactants have become popular in soil flushing due to their biodegradability, low toxicity, effectiveness as well as enhanced biodegradation of organic contaminants [19]. Because the effect of bio-surfactant on the oxygen mass transfer remains important, but at the same time, an unexplored scientific area [20,21], it is of great significance to study the effect of bio-surfactant on the oxygen mass transfer during MNB aeration.

In this work, sodium dodecyl benzene sulfonate (SDBS), triton X-100 (TX-100), rhamnolipid (RHA) and saponin (SAP) were used as surfactants. More specifically, the selected chemical surfactants (SDBS and TX-100) and bio-surfactants (RHA and SAP) are the most frequently used in soil flushing. The research focused on studying the effect of surfactants on the oxygen mass transfer in MNB aeration systems. For this purpose, bubble diameter (d_i), gas holdup (ε) and volumetric mass-transfer coefficient (k_La) were measured and analyzed with respect to different concentrations and types of surfactants. Then, the k_L was calculated in each aqueous surfactant solution and compared with correlations of Frössling's and Sardeing's models for predicting the oxygen mass transfer.

2. Experimental

2.1. Materials

Compressed oxygen and nitrogen with the concentration of 99.9% each were used as the gas phases in this research. Deionized water was used to make aqueous surfactant solutions. Surfactants used in this research consisted of anionic surfactants (SDBS (AR, CAS: 25155-30-0) and RHA (95% (mass), CAS: 147858-26-2)) and non-ionic surfactant (TX-100 (CP, CAS: 9002-93-1) and SAP (60% (mass), CAS: 8047-15-2)), which were purchased from Macklin Biochemical Technology Co., Ltd (Shanghai, China). Specifically, bio-surfactants included RHA and SAP, while the chemical surfactants included SDBS as well as TX-100. Table 1 lists various aqueous solutions prepared with different concentrations of surfactants. The critical micellar concentration (CMC) of these four surfactants as well as the density (ρ_L), dynamic viscosity (μ_L), static surface tension (σ_L) and pH value of aqueous surfactant solutions are presented in Table S1 of the Supplementary Appendix.

2.2. Methods

The experimental setup used in this study was identical to that previously described for the study of oxygen mass transfer in an MNB column [22]. Fig. 1 shows the schematic of the experimental setup used in the current work. The bubble column had an inner diameter of 260 mm and a height of 650 mm. An MNB generator (XZCP-K-1.1, Yunnan Xiazhichun Environmental Protection Technology Co., Ltd., China) of pressurized dissolution type was used to generate MNB in the experiments. A dissolved oxygen (DO) meter (YSI ProSolo, USA) was immersed in the liquid phase to measure the time-dependent DO concentration. A ruler ($h \pm 0.1$ mm) was attached to the outer wall of the bubble column to measure the change in liquid height during the MNB aeration process.

Prior to the MNB aeration process, several rinsing cycles were carried out for the cleaning of vessels. The experiments were conducted at a controlled temperature of 25 °C. For the MNB aeration process, 20 L of deionized water or aqueous surfactant solution at 25 °C was fed into the bubble column. The solution was de-aerated by purging with nitrogen until only a minimum level of DO (0.2 mg·L^{-1}) remained in the vessel. Finally, when the nitrogen bubbles disappeared, the MNB was generated with the oxygen flow rate of 1.8 L·min^{-1} and the solution flow rate of 20 L·min^{-1}. All MNB aeration experiments were conducted in triplicate, and the standard deviation was less than 15% in all cases.

Before MNB aeration, a ruler ($h \pm 0.1$ mm) was inserted into the liquid to measure the liquid height at three different positions in the bubble column. The same procedure was applied to measure the liquid level after MNB aeration. The difference of liquid height before and after the MNB generation (h_0, h) was used to determine gas holdup (ε). During MNB aeration, the concentration of DO in the solution (C^*) was monitored continuously using the DO meter. The meter could read DO within the range of 0–50 mg·L^{-1} with the accuracy of ±0.1 mg·L^{-1}, whereas the reading frequency was one reading every 2 s. The total time of measurement for oxygen was long enough to reach the saturation concentration. After the MNB aeration, the bubble diameter (d_i) of MNB and the volume percentage of MNB with different values of d_i were immediately measured using a particle–size analyzer (Microtrac S3500, USA). This analyzer allowed the detection of bubbles within the range of 0.01–2800 μm. The diffusion coefficient of oxygen (D) in the surfactant solution was measured at the free gas-liquid interface, and the specific methodology used to obtain these parameters is described in the previous studies [23].

3. Results and Discussion

3.1. Effect of surfactants on the interfacial area

Sauter mean diameter of bubble (d_{BS}) is calculated by Eq. (1) [24].

$$d_{BS} = \frac{\sum n_i d_i^3}{\sum n_i d_i^2} \tag{1}$$

where d_i is the bubble diameter and n_i is the number of bubbles within the bubble diameter range of d_i. Fig. 2 shows the effect of surfactants on the value of d_{BS} of MNB. In deionized water, the d_{BS} of bubble was 45.53 μm. It has been found that MNB is negatively charged and stable for long periods of time in liquid [25]. In the surfactant solution, the increase in surfactant concentration reduced the value of d_{BS}. This was due to the fact that the mobility on the surface of bubbles was restricted by the development of surface tension gradient [26]. For this reason, the surface of bubbles could be considered immobile and the rate of film thinning became very small. In addition, the surfactant molecules adsorbed on the gas–liquid interface with the hydrophobic surfactant moieties orientated towards the gas bubbles, whereas the

Table 1
Concentrations of surfactants used in the current work

Aqueous solutions		c/mol·L^{-1}	c/g·L^{-1}	c/CMC	Aqueous solutions		c/mol·L^{-1}	c/g·L^{-1}	c/CMC
Anionic surfactant	SDBS	1.3602×10^{-4}	0.0474	0.025	Non-ionic surfactant	TX-100	2.396×10^{-5}	0.0155	0.200
		6.8010×10^{-4}	0.2370	0.125			1.1981×10^{-4}	0.0775	1.000
		1.36019×10^{-3}	0.4740	0.250			2.3962×10^{-4}	0.1550	2.000
		5.44077×10^{-3}	1.8960	1.000			9.5848×10^{-4}	0.6200	8.000
		8.16116×10^{-3}	2.8440	1.500			1.43771×10^{-3}	0.9300	12.000
	RHA	0.570×10^{-5}	0.0035	0.025		SAP	6.039×10^{-5}	0.0250	0.025
		2.849×10^{-5}	0.0175	0.125			3.0193×10^{-4}	0.1250	0.125
		5.698×10^{-5}	0.0350	0.250			6.0386×10^{-4}	0.2500	0.250
		2.2790×10^{-4}	0.1400	1.000			2.41546×10^{-3}	1.0000	1.000
		3.4185×10^{-4}	0.2100	1.500			3.62319×10^{-3}	1.5000	1.500

Note: The concentration of surfactant is abbreviated as c, while the ratio of c to CMC is abbreviated as c/CMC.

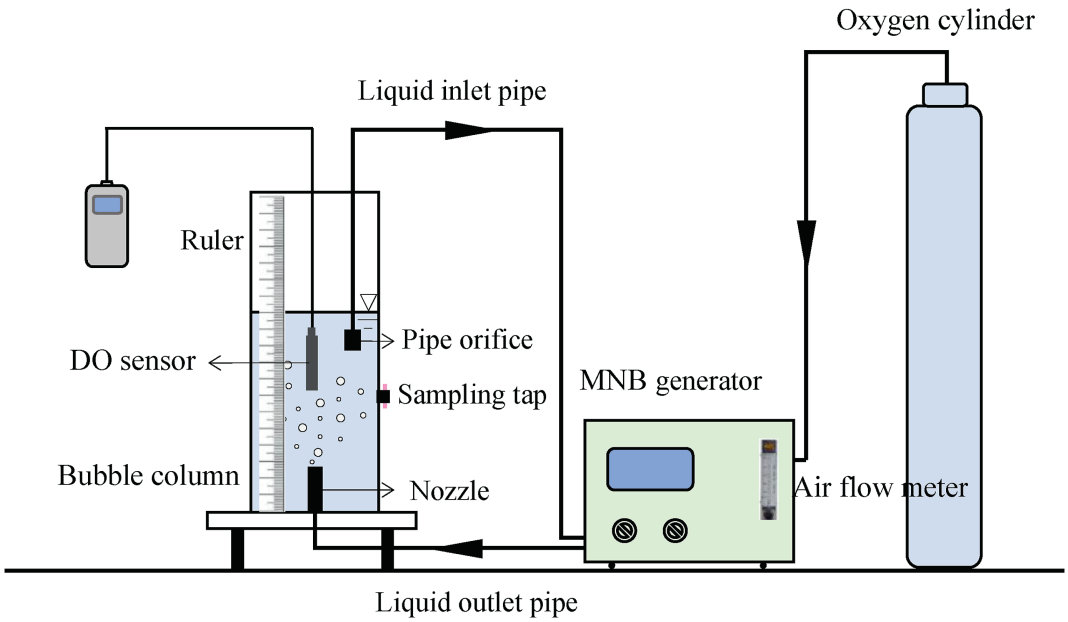

Fig. 1. Schematic of the experimental setup used in the current work [22].

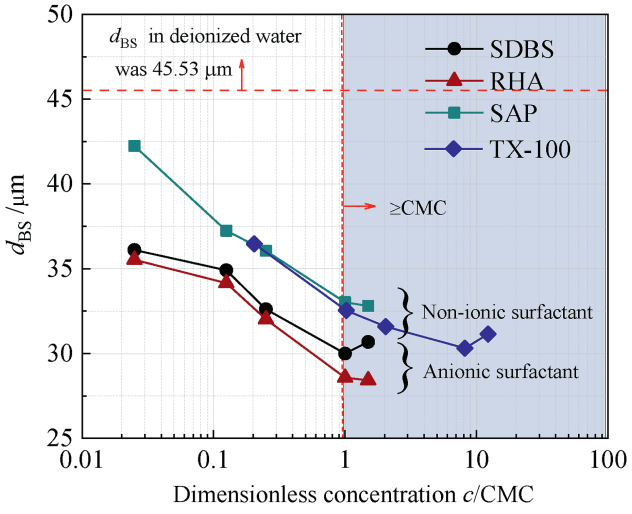

Fig. 2. Effects of surfactants on the bubble diameter.

hydrophilic surfactant moieties orientated towards the bulk liquid. Due to this reason, the bubble coalescence was hindered and the bubble stability was enhanced [27]. The simultaneous effect of immobile bubble surface and suppression of coalescence led to the generation of smaller bubbles in the surfactant solution. As shown in Fig. 2, the d_{BS} of bubbles in the surfactant solution with the c/CMC of less than 1 was larger than that of bubbles in the surfactant solution with the c/CMC of greater than 1. The reason for this phenomenon was that, when c/CMC was less than 1, the surfactant concentration at the gas–liquid interface did not reach the maximum value. For the low concentrations of the surfactant, the coalescence suppression effect increased significantly with the increase in surfactant concentration [28]. This means that the amount of surfactant was not large enough to completely prevent the coalescence of bubbles when c/CMC was less than 1. As the value of c/CMC increased, the value of d_{BS} decreased. When the c/CMC was higher than 1 and the σ_L of surfactant solution remained at a constant value (Table S1 in Supplementary Material), the value of d_{BS} kept on decreasing. The number of surfactant molecules also played a crucial role in decreasing of the value of d_{BS}. In addition, it can also be seen from Fig. 2 that, for anionic surfactant solutions of SDBS or RHA, the value of d_{BS} decreased when the value of c/CMC increased to 1, and this was accompanied by an overall reduction in the mean size of bubble from 45 to 30 μm. In the case of non-ionic surfactant solutions of TX-100 or SAP, there was also recognizable decrease in the value of d_{BS} with the increase in the value of c/CMC to 1. There was a quite larger drop in d_{BS} for anionic

surfactant solution than non-ionic surfactants. This difference between the anionic and non-ionic surfactant solutions suggests that the surface charge is an important factor during the production of MNB. In ionic surfactant solutions, repulsive forces were developed between the MNB due to the presence of electric charge, which was similar to the case of salt solutions [27]. Coalescence in ionic surfactant solution was inhibited to a greater extent than the non-ionic surfactant solution. Therefore, smaller bubbles appeared in the anionic surfactant solutions.

Gas holdup (ε) can be calculated using Eq. (2) [29].

$$\varepsilon = \frac{h - h_0}{h} \tag{2}$$

where h_0 and h are the liquid heights before and after the MNB aeration process, respectively. After MNB aeration, there was a thick layer of foam in the surfactant solution with high concentration of surfactant. Therefore, the value of ε in SDBS solutions (5.44077×10^{-3} and 8.16116×10^{-3} mol·L^{-1}), RHA solutions (5.698×10^{-5}, 2.2790×10^{-4} and 3.4185×10^{-4} mol·L^{-1}), TX-100 solutions (1.1981×10^{-4}, 2.3962×10^{-4}, 9.5848×10^{-4} and 1.43771×10^{-3} mol·L^{-1}) and SAP solutions (3.0193×10^{-4}, 6.0386×10^{-4}, 2.41546×10^{-3} and 3.62319×10^{-3} mol·L^{-1}) were not obtained in the experiment. On the contrary, foam did not appear in the surfactant solution with low concentration. Therefore, the ε in low-concentration surfactant solution could be obtained using Eq. (2) and the corresponding results are shown in Fig. 3. It could be observed that, regardless of the surfactant type and concentration, the presence of surfactant resulted in an increase in the value of ε. The main reason for this phenomenon was that d_{BS} for surfactant solution was less than for deionized water (Fig. 2), due to which, the bubble rise velocity in the surfactant solution was smaller than that in deionized water. It is also worth noticing that the ε in SDBS or RHA solutions was higher than that in TX-100 or SAP solutions. The difference may be attributed to the electric charge of ionic surfactants [30]. As discussed above, electric charge potentially reduced the coalescence by increasing the repulsive forces among MNB. Smaller and numerous bubbles appeared in the anionic surfactant solutions compared to those in the non-ionic surfactant solutions. Therefore, the value of ε in anionic surfactant solutions was larger than that in the non-ionic surfactant solutions.

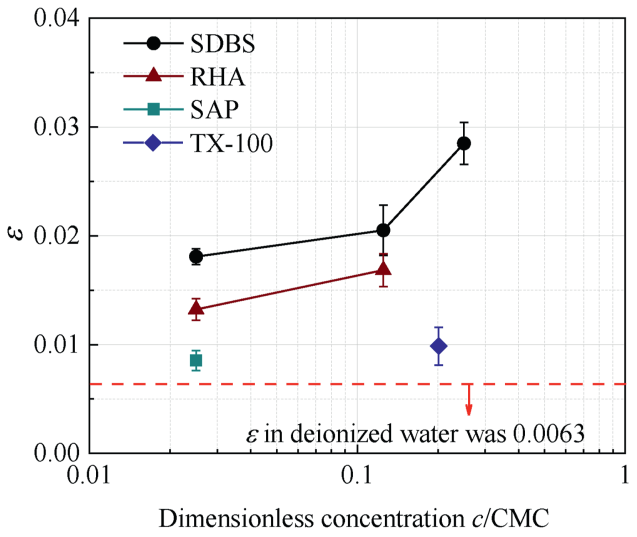

Fig. 3. Effects of surfactant on gas hold-up (ε).

3.2. Effect of surfactant on the mass transfer parameters

For the experimental apparatus in this research, it is worth noting that oxygen absorption occurred in the bubble column, MNB generator and connecting pipes. Furthermore, the mass transfer rate was not uniform in the bubble column. Therefore, the value of k_La in this research represented the local volumetric liquid-side mass-transfer coefficient in the experimental apparatus including bubble column, MNB generator and connection pipes. The effect of surfactant on the value of k_La is shown in Fig. 4. The results showed that, whatever the liquid phase was, the k_La value decreased with the increase of surfactant concentration. Additionally, this variation trend was more obvious when the value of c/CMC was less than 1. This meant that the presence of surfactant, even in small amounts, had significant effect on the mass transfer mechanism. Furthermore, the effect of non-ionic surfactant on the value of k_La was greater than that of ionic surfactant. Moreover, RHA with the high molecular weight had a more noticeable inhibitory effect than SDBS. These results showed that the type and concentration of surfactant had a direct effect on the oxygen mass transfer during MNB aeration process. To understand these phenomena properly, the gas–liquid interfacial area (a) and liquid-side mass-transfer coefficient (k_L) had to be considered separately.

It is worth mentioning here that the value a can be obtained from the values of d_{BS} and ε using Eq. (3) [31].

$$a = \frac{6\varepsilon}{d_{BS} \times (1 - \varepsilon)} \tag{3}$$

The effect of surfactant on the value of a is shown in Fig. 5. The values of a increased with the increase of surfactant concentration. The increase was attributed to the increase of ε (Fig. 3) and the decrease of d_{BS} (Fig. 2). With large value of a and longer oxygen mass transfer time (small bubble rise velocity), MNB in the surfactant solution should have a very high k_La value. However, the k_La values in the surfactant solutions were lower than those in the deionized water (Fig. 4). This phenomenon was mainly related to the change of k_L in the surfactant solution.

It is worth mentioning that the value of k_L can be obtained from the values of k_La and a using Eq. (4).

$$k_L = \frac{k_La}{a} \tag{4}$$

The k_L in different surfactant solutions can be calculated using Eq. (4), and the results are shown in Fig. 6. It can be seen from Fig. 6

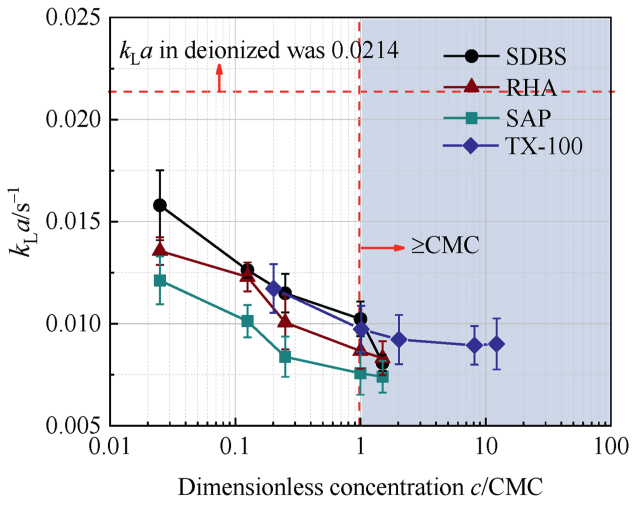

Fig. 4. Effects of surfactant on the volumetric mass-transfer coefficient (k_La).

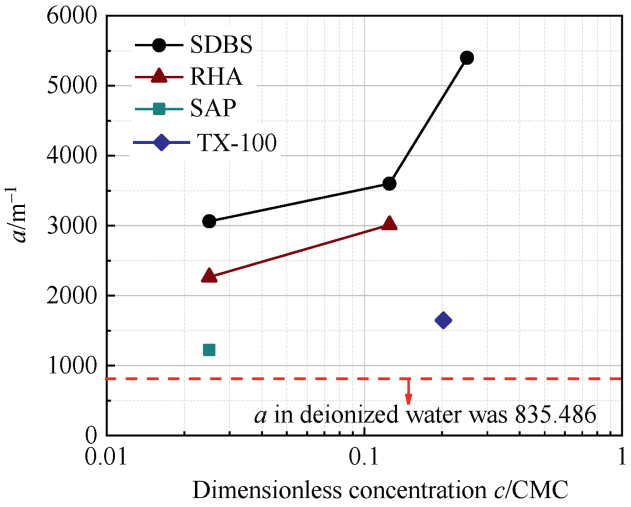

Fig. 5. Effects of surfactant on the gas–liquid interfacial area (a).

that the value of k_L for the surfactant solution was lower than that for the deionized water. The low k_L value in surfactant solution was attributed to modifications of gas–liquid interface caused by the accumulation of surfactant molecules. The accumulation led to a reduction in the renewal of liquid elements, resulting in a decrease in the value of driving force [32]. In addition, the accumulation increased the liquid-phase mass transfer resistance. Therefore, k_L in the surfactant solution was less than that in deionized water. It also can be seen from Fig. 6 that the reduction in the value of k_L in the anionic surfactant solution (SDBS or RHA) was greater than that in the non-ionic surfactant solution (TX-100 or SAP). This was closely related to the d_{BS} of MNB. More specifically, MNB in anionic surfactant solution had smaller bubble diameter than in the non-ionic surfactant solution. Smaller MNB had quite lower interfacial renewal velocity, and once the surfactants had been adsorbed to the surface, their hydrophobic tails inside the MNB would reduce the internal gas circulation. In addition, surfactant molecules accumulated at the bottom of MNB, creating a stagnation zone inside the bubble [14]. These effects produced a significant decrease in the value of k_L in the anionic surfactant solution. As shown in Fig. 6, the two anionic surfactants (SDBS and RHA) displayed different effects on the value of k_L. The molecular weight of the surfactant can be used to explain this phenomenon. The low-molecule weight

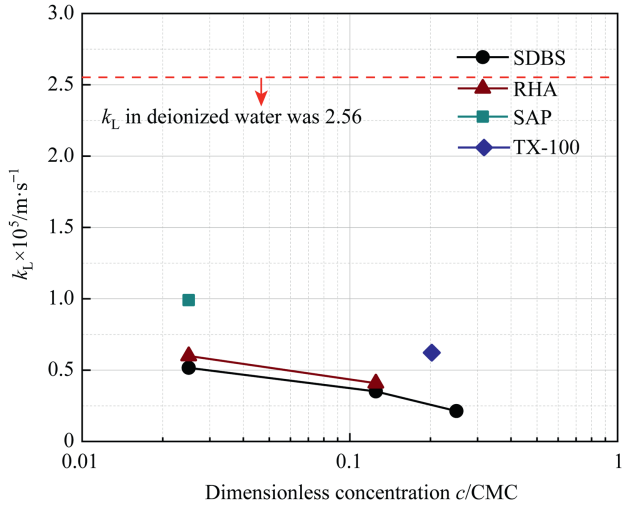

Fig. 6. Effects of surfactant on the liquid-side mass-transfer coefficient (k_L).

surfactant migrates faster towards the bubble surface than the high-molecular weight surfactant [4]. Due to this reason, SDBS with low molecular weight had a more noticeable inhibitory effect than RHA.

3.3. Evaluation of the mass transfer model

In most studies, slip velocity models were used to analyze the absorption process in bubble columns. Slip velocity models assume a gross mean flow of fluid with respect to the bubble (slip velocity), and this behavior develops a greater renewal of the liquid at the bubble surface because of the bubble surface mobility rather than the small-scale eddies of turbulent fields [33]. Regarding these models, the models proposed by Calderbank and Moo-Young [34] and Frössling [35] have been employed in the last few years. These models are applicable to gas–liquid systems with small bubbles having diameters of less than 1.5 mm, or contaminated bubbles with surface contaminants such as surfactants. The model developed by Frössling is given by Eq. (5) [35].

$$k_L^{\text{Frossling}} = 0.6\sqrt{\frac{v_s}{d_{BS}}}D^{2/3}\nu^{-1/6} \tag{5}$$

where v_s is the slip velocity. In bubble columns, slip velocity is assumed to be close to the single bubble terminal velocity (v_t) [36]. In the current research, v_t can be calculated using Stokes' law [27] (Eq. (S1) in the Supplementary Material). Table S2 summarizes the values of v_t in different surfactant solutions. Moreover, D is the diffusion coefficient of oxygen in the surfactant solution, as presented in Table S1, and υ is the kinematic viscosity of aqueous surfactant solutions.

In addition, Sardeing *et al.* [11] developed a model, which took into account the presence of surface-active substances in gas–liquid interface, as well as the surface activity and diffusivity values corresponding to the solutes used to make the solutions. When an adsorption step is involved in a global process, Langmuir isotherm is commonly employed, which is given by Eq. (6).

$$S_e = \frac{\Gamma_e}{\Gamma_\infty} = \frac{Kc}{1+Kc} \tag{6}$$

where S_e is the surface coverage ratio at equilibrium, c is the concentration of surfactant, and Γ_∞ and Γ_e are the surface concentrations at saturation and equilibrium, respectively. Furthermore, K is the adsorption equilibrium constant of surfactant, as presented in Table S3. Eq. (6) can be used to determine the value of the surface coverage ratio and the influence of the surfactant concentration. In Eq. (6), $S_e = 0$ corresponds to an interface free of surfactants (deionized water in this work), whereas $0 < S_e < 1$ corresponds to a non-saturated interface (low concentration of surfactant). Moreover, the condition of $S_e = 1$ in Eq. (6) corresponds to an interface saturated with surfactants.

For the specific experimental conditions employed in the current research, the predicted value of k_L using this model must be controlled between two limits, namely the mass-transfer coefficient for a free surface ($S_e = 0$) (k_L^0), and the mass transfer for a saturated surface ($S_e = 1$) (k_L^1). According to these conditions, the Sardeing's model for estimating the value of k_L can be expressed as Eq. (7).

$$k_L^{\text{Sardeing}} = S_e k_L^1 + (1 - S_e)k_L^0 \tag{7}$$

Under the present experimental conditions, k_L^0 could be determined using Frössling's model (Eq. (5)). Furthermore, k_L^1 corresponding to a saturated interface could be calculated by Eq. (8) [11].

$$k_L^1 = 1.744K^{-0.084}k_L^{\text{Frossling}} \quad (8)$$

where $k_L^{\text{Frossling}}$ represents the value of k_L calculated using Frössling's model.

Fig. 7 shows the comparison between the experimental and predicted values of k_L using Sardeing's or Frössling's model. In deionized water, the predicted k_L values of the two models were higher than the experimental k_L values. This may be due to the diameter of MNB. More specifically, the Frössling's model was used to predict the k_L of bubble with the diameter of less than 1.5 mm, and Frössling's model was based on the bubble with the diameter of a few hundreds of a micron. However, the bubble diameter in this research lied within the range of 25–50 μm. The renewal of the liquid elements at the smaller MNB interface was different from that at normal MNB. Therefore, the experimental k_L values were different from the k_L values predicted using the Sardeing's or Frössling's model. In aqueous surfactant solutions, the predicted k_L values by the two models were also higher than the experimental k_L values. As discussed above, the accumulation of surfactant at the smaller MNB interface was more conspicuous than at normal MNB. The bubble size in this research was less than that in the research of Sardeing *et al.* [11] and Frössling [35]. This means that the Sardeing's or Frössling's model was not suitable for predicting the k_L value of the MNB aeration system.

In order to estimate the k_L value in the MNB aeration system, the Frössling's model has to be modified. More specifically, the ratio of the experimental values to calculated ones using Frössling's model is introduced, as given by Eq. (9).

$$f_c = \frac{k_L^{\text{Experimental}}}{k_L^{\text{Frossling}}} \quad (9)$$

In addition, *Z*, the Ohnesorge number, is given by Eq. (10).

$$Z = \frac{\mu_L}{(\rho_L d_{BS}\sigma_L)^{0.5}} \quad (10)$$

where μ_L is the dynamic viscosity, σ_L is the static surface tension, and ρ_L is the density. In order to find the relationship between f_c and *Z*, the values of $k_L^{\text{Experimental}}$ (as shown in Fig. 6), $k_L^{\text{Frossling}}$ as shown in Fig. 7), d_{BS} (as shown in Fig. 2), μ_L, ρ_L and σ_L (obtained from Table S1) were used to calculate the values of f_c and *Z* using Eqs. (9) and (10), respectively. As shown in Fig. 8, the values of f_c were plotted against those of *Z* in Fig. 8.

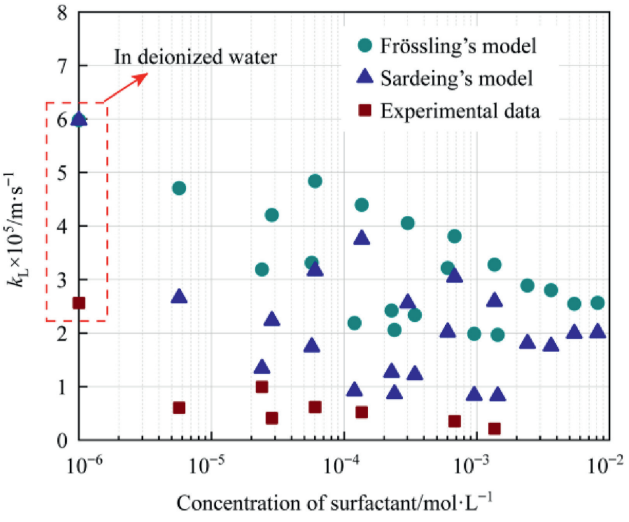

Fig. 7. Comparisons of the experimental and predicted k_L values using Sardeing's or Frössling's model.

In Fig. 8, the f_c can be correlated with *Z* using Eq. (11).

$$f_c = 8.542 \times 10^{-10} \cdot Z^{-4.79} \quad (11)$$

According to Eq. (9), k_L can be calculated using Eq. (12).

$$k_L^{\text{Experiment}} = f_c \cdot k_L^{\text{Frossling}} \quad (12)$$

The modified Frössling's model is given by Eq. (13).

$$k_L^{\text{Modified Frossling}} = f_c \cdot k_L^{\text{Frossling}} \quad (13)$$

According to Eqs. (11) and (13), $k_L^{\text{Modified Frossling}}$ can be calculated using Eq. (14).

$$k_L^{\text{Modified Frossling}} = 8.542 \times 10^{-10} \cdot Z^{-4.79} \cdot k_L^{\text{Frossling}} \quad (14)$$

The modified Sardeing's model can be expressed using Eq. (15).

$$k_L^{\text{Modified Sardeing}} = S_e k_L^1 + (1 - S_e)k_L^0 \quad (15)$$

where k_L^0 can be calculated by the modified Frössling's model (Eq. (14)). Based on Eqs. (8) and (14), k_L^1 can be calculated using Eq. (16).

$$k_L^1 = 1.744K^{-0.084}k_L^{\text{Modified Frossling}} \quad (16)$$

Fig. 9 shows the comparison of experimental k_L values and the k_L values predicted using the modified Sardeing's or Frössling's model. It is clear that the values calculated using modified Frössling's model agreed with the most of experimental values within ±20%. There was a deviation between the experimental k_L values and the values of k_L predicted using the modified Sardeing's model. According to Sardeing *et al.* [11], the k_L^1 values depended on the type of surfactant. Moreover, Eq. (8) was obtained based on the experimental data in the research of Sardeing *et al.* [11]. However, the surfactants used in the current research were different from the surfactant employed in their research. Therefore, the modified Sardeing's model did not describe the variation in the experimental k_L values. In addition, the difference between the experimental and predicted k_L values clearly confirmed the need to complete the empirical and/or theoretical correlations for determining k_L in MNB aeration systems. This condition is imperatively required to describe and appropriately model the oxygen mass transfer.

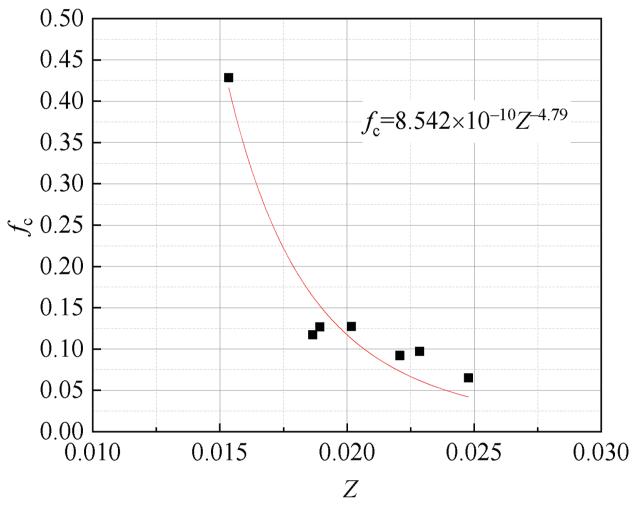

Fig. 8. Correlation between f_c and *Z*.

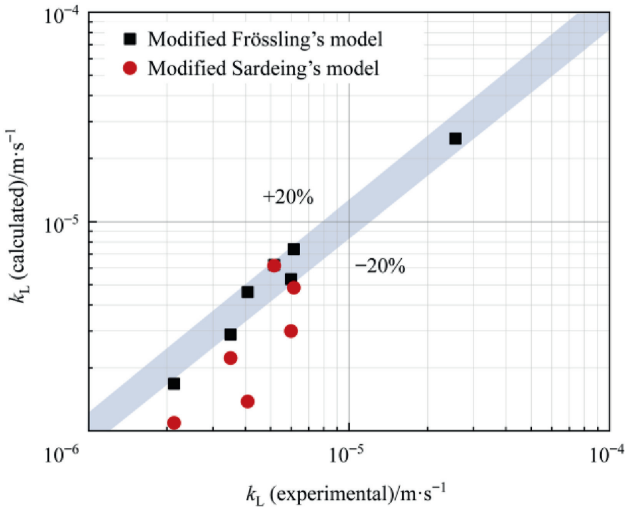

Fig. 9. Comparisons of the experimental k_L values and those predicted using modified Sardeing's or Frössling's model.

4. Conclusions

In this work, chemical surfactant and bio-surfactant, which are the most frequently used in soil flushing, were used to study the effect of surfactant on the oxygen mass transfer in an MNB aeration system. Firstly, bubble diameter and gas holdup were measured to study the effect of surfactant on the interfacial area. Then, volumetric mass-transfer coefficient and liquid-side mass-transfer coefficient were calculated to analyze the effect of surfactant on the mass transfer parameters. Finally, modified Sardeing's and Frössling's models were employed to fit the experimental liquid-side mass-transfer coefficient data. Based on the test results, the following conclusions are drawn.

(1) Due to the immobile bubble surface and the suppression of coalescence effect, there was a decrease in the value of d_{BS} and an increase in ε in the surfactant solutions. These variation trends were more obvious at higher surfactant concentrations. Furthermore, with the presence of electric charge, smaller and more MNB appeared in the anionic surfactant solutions than in the non-ionic surfactant solutions, thereby the value of ε in the anionic surfactant solutions was higher than that in the non-ionic surfactant solutions.
(2) Because of the accumulation of surfactant on the MNB surface, the k_La and k_L values decreased with the increase of surfactant concentration. In addition, due to the small MNB in anionic surfactant solutions, and the reason that the accumulation of surfactant at smaller MNB interface was more conspicuous than at bigger MNB, the hindrance effect of ionic surfactants on the k_L was greater than that of non-ionic surfactants.
(3) Whether in deionized water or surfactant solution, the Sardeing's or Frössling's model was not suitable for predicting the value of k_L in MNB aeration. Although the modified Frössling's model described the effect of surfactant on k_L in MNB aeration system, it is necessary to complete the empirical and/or theoretical correlations for determining k_L in the MNB aeration systems.

Declaration of Interests

The authors declare that they have no known competing financial interests or personal relationships that could have appeared to influence the work reported in this paper.

Acknowledgements

This research was financially supported by the National Natural Science Foundation of China (41877240), National Key Research and Development Program of China (2018YFC1802300) and Scientific Research Foundation of Graduate School of Southeast University (YBPY2154).

Supplementary Material

Supplementary data to this article can be found online at https://doi.org/10.1016/j.cjche.2023.11.009.

Nomenclature

a	gas–liquid interfacial area, L·m^{-1}
C	concentration of surfactant, mol·L^{-1}
C^*	DO concentration at time t, g·m^{-3}
D	diffusion coefficient of oxygen in the surfactant solution, m^2·s^{-1}
d_{BS}	Sauter mean diameter of bubble, m
d_i	bubble diameter, m
h	liquid height after MNB aeration, m
h_0	liquid height before MNB aeration, m
K	adsorption equilibrium constant of surfactant
k_L	liquid-side mass-transfer coefficient, m·s^{-1}
k_La	volumetric mass-transfer coefficient, s^{-1}
k_L^0	k_L for a free surface ($S_e = 0$), m·s^{-1}
k_L^1	k_L for a saturated surface ($S_e = 1$), m·s^{-1}
$k_L^{Frossling}$	k_L is calculated by Frössling's model, m·s^{-1}
$k_L^{Modified\ Frossling}$	k_L is calculated by modified Frössling's model, m·s^{-1}
$k_L^{Modified\ Sardeing}$	k_L is calculated by modified Sardeing's model, m·s^{-1}
$k_L^{Sardeing}$	k_L is calculated by Sardeing's model, m·s^{-1}
S_e	surface coverage ratio at equilibrium
Γ_e	surface concentration at equilibrium, mol·L^{-1}
Γ_∞	surface concentration at saturation, mol·L^{-1}
v_s	slip velocity, m·s^{-1}
v_t	terminal velocity of single bubble, m·s^{-1}
ε	gas holdup
μ_L	dynamic viscosity of aqueous surfactant solution, Pa·s
ρ_L	density of aqueous surfactant solution, kg·m^{-3}
σ_L	static surface tension of aqueous surfactant solution, N·m^{-1}
υ	kinematic viscosity of aqueous surfactant solution, m^2·s^{-1}

References

[1] F.I. Khan, T. Husain, R. Hejazi, An overview and analysis of site remediation technologies, *J. Environ. Manag.* 71 (2) (2004) 95–122.
[2] Z. Rahman, An overview on heavy metal resistant microorganisms for simultaneous treatment of multiple chemical pollutants at co-contaminated sites, and their multipurpose application, *J. Hazard Mater.* 396 (2020) 122682.
[3] C.N. Mulligan, Sustainable remediation of contaminated soil using bio-surfactants, *Front. Bioeng. Biotechnol.* 9 (2021) 635196.
[4] D. Rosso, D.L. Huo, M.K. Stenstrom, Effects of interfacial surfactant contamination on bubble gas transfer, *Chem. Eng. Sci.* 61 (16) (2006) 5500–5514.
[5] S.S. Alves, S.P. Orvalho, J.M.T. Vasconcelos, Effect of bubble contamination on rise velocity and mass transfer, *Chem. Eng. Sci.* 60 (1) (2005) 1–9.
[6] J.M.T. Vasconcelos, S.P. Orvalho, S.S. Alves, Gas–liquid mass transfer to single bubbles: Effect of surface contamination, *AIChE J.* 48 (6) (2002) 1145–1154.
[7] Q. Han, X.Y. Zhang, H.B. Wu, X.T. Zhou, H.B. Ji, Different efficiency toward the biomimetic aerobic oxidation of benzyl alcohol in microchannel and bubble column reactors: Hydrodynamic characteristics and gas–liquid mass transfer, *Chin. J. Chem. Eng.* 55 (2023) 84–92.
[8] P. Painmanakul, G. Hébrard, Effect of different contaminants on the α-factor: Local experimental method and modeling, *Chem. Eng. Res. Des.* 86 (11) (2008) 1207–1215.

[9] A.C. Ahmia, M. Idouhar, K. Wongwailikit, N. Dietrich, G. Hébrard, Impact of cellulose and surfactants on mass transfer of bubble columns, *Chem. Eng. Technol.* 42 (11) (2019) 2465–2475.
[10] P. Painmanakul, K. Loubière, G. Hébrard, M. Mietton-Peuchot, M. Roustan, Effect of surfactants on liquid-side mass transfer coefficients, *Chem. Eng. Sci.* 60 (22) (2005) 6480–6491.
[11] R. Sardeing, P. Painmanakul, G. Hébrard, Effect of surfactants on liquid-side mass transfer coefficients in gas–liquid systems: A first step to modeling, *Chem. Eng. Sci.* 61 (19) (2006) 6249–6260.
[12] D. Rosso, M.K. Stenstrom, Surfactant effects on alpha-factors in aeration systems, *Water Res.* 40 (7) (2006) 1397–1404.
[13] G.H. Kelsall, S.Y. Tang, A.L. Smith, S. Yurdakul, Measurement of rise and electrophoretic velocities of gas bubbles, *J. Chem. Soc., Faraday Trans.* 92 (20) (1996) 3879–3885.
[14] F.H. Garner, D. Hammerton, Circulation inside gas bubbles, *Chem. Eng. Sci.* 3 (1) (1954) 1–11.
[15] S.J. Lee, S. Kim, Simultaneous measurement of size and velocity of microbubbles moving in an opaque tube using an X-ray particle tracking velocimetry technique, *Exp. Fluid* 39 (3) (2005) 492–497.
[16] L. Parkinson, R. Sedev, D. Fornasiero, J. Ralston, The terminal rise velocity of 10–100 microm diameter bubbles in water, *J. Colloid Interface Sci.* 322 (1) (2008) 168–172.
[17] B. Cuenot, J. Magnaudet, B. Spennato, The effects of slightly soluble surfactants on the flow around a spherical bubble, *J. Fluid Mech.* 339 (1997) 25–53.
[18] F. Takemura, Adsorption of surfactants onto the surface of a spherical rising bubble and its effect on the terminal velocity of the bubble, *Phys. Fluids* 17 (4) (2005) 048104.
[19] Y.X. Yu, J. Zhao, A.E. Bayly, Development of surfactants and builders in detergent formulations, *Chin. J. Chem. Eng.* 16 (4) (2008) 517–527.
[20] H. Amani, Application of a dynamic method for the volumetric mass transfer coefficient determination in the scale-up of rhamnolipid biosurfactant production, *J. Surfactants Deterg.* 21 (6) (2018) 827–833.
[21] M. Rezaei, G. Moussavi, K. Naddafi, M.S. Johnson, Enhanced biodegradation of styrene vapors in the biotrickling filter inoculated with biosurfactant-generating bacteria under H_2O_2 stimulation, *Sci. Total Environ.* 704 (2020) 135325.
[22] M. Bai, Z.B. Liu, J.P. Zhang, L.L. Lu, Prediction and experimental study of mass transfer properties of micronanobubbles, *Ind. Eng. Chem. Res.* 60 (22) (2021) 8291–8300.
[23] M. Bai, Z.B. Liu, L.T. Zhan, Z.H. Fan, M.X. Yuan, Z. Liu, Effect of chemical agents on the diffusion behavior of oxygen in groundwater under combined remediation technique of air sparging and soil flushing, *Water Air Soil Poll* 234 (2023) 680.
[24] A. Kawahara, M. Sadatomi, F. Matsuyama, H. Matsuura, M. Tominaga, M. Noguchi, Prediction of micro-bubble dissolution characteristics in water and seawater, *Exp. Therm. Fluid Sci.* 33 (5) (2009) 883–894.
[25] M. Takahashi, K. Chiba, P. Li, Free-radical generation from collapsing microbubbles in the absence of a dynamic stimulus, *J. Phys. Chem. B* 111 (6) (2007) 1343–1347.
[26] G. Marrucci, A theory of coalescence, *Chem. Eng. Sci.* 24 (6) (1969) 975–985.
[27] B. Swart, Y.B. Zhao, M. Khaku, E. Che, R. Maltby, Y.M. John Chew, J. Wenk, *In situ* characterisation of size distribution and rise velocity of microbubbles by high-speed photography, *Chem. Eng. Sci.* 225 (2020) 115836.
[28] H. Zhang, Y. Wang, T. Wang, Experimental study on effect of alcohol surfactants on bubble coalescence in full range of concentrations, *CIESC J* 71 (9) (2020) 4161–4167. (in Chinese)
[29] K. Muroyama, K. Imai, Y. Oka, J. Hayashi, Mass transfer properties in a bubble column associated with micro-bubble dispersions, *Chem. Eng. Sci.* 100 (2013) 464–473.
[30] K. Tse, T. Martin, C.M. McFarlane, A.W. Nienow, Visualisation of bubble coalescence in a coalescence cell, a stirred tank and a bubble column, *Chem. Eng. Sci.* 53 (23) (1998) 4031–4036.
[31] M. Tobajas, E. García-Calvo, M.H. Siegel, S.E. Apitz, Hydrodynamics and mass transfer prediction in a three-phase airlift reactor for marine sediment biotreatment, *Chem. Eng. Sci.* 54 (21) (1999) 5347–5354.
[32] D. Gómez-Díaz, J.M. Navaza, B. Sanjurjo, Mass-transfer enhancement or reduction by surfactant presence at a gas–liquid interface, *Ind. Eng. Chem. Res.* 48 (5) (2009) 2671–2677.
[33] V. Linek, M. Kordač, M. Fujasová, T. Moucha, Gas–liquid mass transfer coefficient in stirred tanks interpreted through models of idealized eddy structure of turbulence in the bubble vicinity, *Chem. Eng. Process* 43 (12) (2004) 1511–1517.
[34] P.H. Calderbank, M.B. Moo-Young, The continuous phase heat and mass-transfer properties of dispersions, *Chem. Eng. Sci.* 16 (1–2) (1961) 39–54.
[35] N. Frössling, The evaporation of falling drops, *Gerl. Beitrage Geophys.* 52 (1938) 170–216.
[36] S.S. Alves, C.I. Maia, J.M.T. Vasconcelos, A.J. Serralheiro, Bubble size in aerated stirred tanks, *Chem. Eng. J.* 89 (1–3) (2002) 109–117.